

Estimation of Thermoelastic State of a Thermally Sensitive Functionally Graded Thick Hollow Cylinder: A Mathematical Model

V.R. Manthana^{1,*}, N.K. Lamba², G.D. Kedar³

¹*Department of Mathematics, Priyadarshini J.L. College of Engineering, Nagpur, India*

²*Department of Mathematics, Shri Lemdeo Patil Mahavidyalaya, Nagpur, India*

³*Department of Mathematics, RTM Nagpur University, Nagpur, India*

Received 11 July 2018; accepted 17 September 2018

ABSTRACT

The object of the present paper is to study temperature distribution and thermal stresses of a functionally graded thick hollow cylinder with temperature dependent material properties. All the material properties except Poisson's ratio are assumed to be dependent on temperature. The nonlinear heat conduction with temperature dependent thermal conductivity and specific heat capacity is reduced to linear form by applying Kirchhoff's variable transformation. Solution for the two dimensional heat conduction equation with internal heat source is obtained in the transient state. The influence of thermo-sensitivity on the thermal and mechanical behavior is examined. For theoretical treatment all physical and mechanical quantities are taken as dimensional, whereas for numerical computations we have considered non-dimensional parameters. A mathematical model is constructed for both homogeneous and nonhomogeneous case. Numerical computations are carried out for ceramic-metal-based functionally graded material (FGM), in which alumina is selected as ceramic and nickel as metal. The results are illustrated graphically.

© 2018 IAU, Arak Branch. All rights reserved.

Keywords : Functionally graded hollow cylinder; Temperature distribution; Thermal stresses; Thermo-sensitivity.

1 INTRODUCTION

DURING the past three decades, Functionally graded materials (FGMs) have drawn considerable attention in the field of structural engineering applications at extremely high temperature. FGMs are generally composed of different materials such as ceramics and metals with continuous and gradual variation across thickness, which reduces the thermal stresses, thereby improving the mechanical durability of the material. Al-Hajri and Kalla [1] developed a new integral transform and its inversion involving combination of Bessel's function as a kernel and used it to solve mixed boundary value problems. Awaji et al. [2] presented a numerical technique for analyzing one-dimensional transient temperature and stress distributions in a stress-relief-type plate of functionally graded ceramic-metal based materials (FGMs), in relation to both the temperature-dependent thermal properties and continuous and gradual variation of the thermo-mechanical properties of the FGM. Ching and Chen [3] investigated the thermomechanical deformation of a functionally graded composite (FGC) in elevated temperature environments by

*Corresponding author.

E-mail address: vkmanthana@gmail.com (V.R. Manthana).

the meshless local Petrov–Galerkin method. Farid et al. [4] studied free vibration analysis of initially stressed thick simply supported functionally graded curved panel resting on two-parameter elastic foundation, subjected in thermal environment using three-dimensional elasticity formulation. Hata [5] studied thermal stresses in a nonhomogeneous medium whose shear modulus and coefficient of thermal expansion are assumed to vary axially. Hosseini and Akhlaghi [6] studied transient thermal stresses in a thick hollow cylinder made of FGM by assuming the material properties to be nonlinear with a power law distribution through the thickness. Kassir [7] investigated thermal stress problems in a thick plate and a semi-infinite body in nonhomogeneous solids. Kumar et al. [8, 9] studied the two dimensional axisymmetric problem of thick circular plate in modified couple stress theory with heat and mass diffusive sources. Kushnir and Protsyuk [10] presented thermal stressed state of a multilayered thermally sensitive cylinders and spheres under the conditions of convective-radiation heat transfer. Kushnir and Popovych [11] analyzed heat conduction problems of thermo-sensitive solids under complex heat exchange. Lamba et al. [12] analyzed the thermoelastic behavior of a hollow cylinder under heating and cooling process. Liew et al. [13] presented an analysis of the thermomechanical behavior of hollow circular cylinders of FGMs. Manthana et al. [14–18] studied temperature effect, bending moments, thermal stresses in FG and nonhomogeneous solids under unsteady temperature distribution. Moosaie [19] presented an exact analytical solution to the axisymmetric heat conduction equation for hollow spherical objects with temperature-dependent thermal conductivity. Moosaie [20] presented an approximate analytical solution to the axisymmetric heat conduction equation for a hollow cylinder made of functionally graded material with temperature-dependent heat conductivity by considering general linear boundary conditions. Noda [21] presented a brief review on thermal stresses in materials with temperature-dependent properties. Peng and Li [22] presented a novel method for analyzing steady thermal stresses in a functionally graded hollow cylinder. The thermal and thermoelastic parameters are assumed to arbitrarily vary along the radial direction of the hollow cylinder. Popovych [23] studied the modeling of heat fields in thermally sensitive plates. Popovych and Garmatii [24] developed analytic-numerical methods of heat-conduction problems for thermo-sensitive bodies with convective heat transfer. Popovych et al. [25–29] proposed a method of solving stationary heat-conduction problems of contacting bodies with coefficient of thermal conductivity that are linear functions of the temperature and the corresponding problems of thermo-elasticity and a hollow cylinder from whose surfaces a convective heat exchange with the external environment occurs. Popovych and Kalynyak [30] proposed a procedure of getting analytic expressions for the description of axisymmetric stationary thermal fields, axisymmetric static or quasi static stress and strain fields in long hollow multilayer cylinders made of thermally sensitive materials with constant normal loads and arbitrary classical conditions of heat exchange specified on the bounding surfaces. Rakocha and Popovych [31] determined stationary temperature distribution in a three-layer infinite hollow cylinder based on the thermo-sensitive body model. Tang [32] presented a simple thermal stress analysis for thin plates which includes temperature dependent thermal mechanical properties and given derivations for the bending of isotropic elastic plates in the presence of a temperature field. Thawait et al. [33] studied the elastic analysis of concave thickness rotating disks made of functionally graded materials. Tripathi et al. [34] discussed a two dimensional generalized thermoelastic problem of a thick circular plate of finite thickness and infinite extent subjected to continuous axisymmetric heat supply and an internal heat generation within the context of generalized thermo-elasticity.

In the present article, we have considered a two-dimensional transient thermoelastic problem of a thick hollow cylinder occupying the space $a \leq r \leq b$, $0 \leq z \leq h$, subjected to sectional heating on the upper surface. The material properties except Poisson's ratio and density are assumed to be temperature dependent. The solutions are obtained in the transient state in the form of Bessel's and trigonometric functions.

2 THERMOELASTIC EQUATIONS

The strain displacement relations and equilibrium conditions are given by [3]

$$e_r = \frac{\partial u}{\partial r}, \quad e_{\theta\theta} = \frac{u}{r}, \quad e_{zz} = \frac{\partial w}{\partial z}, \quad e_{rz} = \frac{1}{2} \left(\frac{\partial u}{\partial z} + \frac{\partial w}{\partial r} \right) \quad (1)$$

$$\frac{\partial \sigma_r}{\partial r} + \frac{\partial \sigma_{rz}}{\partial z} + \frac{\sigma_r - \sigma_{\theta\theta}}{r} = 0, \quad \frac{\partial \sigma_{rz}}{\partial r} + \frac{\partial \sigma_{zz}}{\partial z} + \frac{\sigma_{rz}}{r} = 0 \quad (2)$$

The stress-strain relations with temperature dependent material properties are formulated as:

$$\begin{aligned} \sigma_{rr} &= 2G(T)e_{rr} + \lambda(T)e - (3\lambda(T) + 2\mu(T))\alpha_r(T)T \\ \sigma_{\theta\theta} &= 2G(T)e_{\theta\theta} + \lambda(T)e - (3\lambda(T) + 2\mu(T))\alpha_r(T)T \\ \sigma_{zz} &= 2G(T)e_{zz} + \lambda(T)e - (3\lambda(T) + 2\mu(T))\alpha_r(T)T \\ \sigma_{rz} &= 2G(T)e_{rz} \end{aligned} \tag{3}$$

where $e_{rr}, e_{\theta\theta}, e_{zz}$ are the strain components ($e = e_{rr} + e_{\theta\theta} + e_{zz}$), $G(T), \lambda(T), \mu(T)$ are shear modulus, Lamé's constants and $\alpha_r(T)$ is the coefficient of thermal expansion. We assume $G(T), \alpha_r(T), \lambda(T)$ and $\mu(T)$ as:

$$\begin{aligned} G(T) &= G_0 \exp(\varpi T), \alpha_r(T) = \alpha_0 \exp(\chi T), \\ \lambda(T) &= \lambda_0 \exp(\varpi T), \mu(T) = \mu_0 \exp(\varpi T), \varpi \leq 0, \chi \geq 0 \end{aligned} \tag{4}$$

where $G_0, \alpha_0, \lambda_0, \mu_0$ are the reference values of shear modulus, coefficient of thermal expansion, Lamé's constant respectively.

Using Eqs. (1), (3) and (4) in (2), the displacement equations of equilibrium are obtained as:

$$\begin{aligned} \nabla^2 u - \frac{u}{r^2} + \frac{1}{G_0\mu_0} \frac{\partial u}{\partial r} \frac{\partial T}{\partial r} + \frac{\lambda_0}{2G_0\mu_0} \frac{\partial e}{\partial r} + \frac{e}{2G_0} \frac{\partial T}{\partial r} - \frac{1}{2} \frac{\partial e_{zz}}{\partial z} + \frac{1}{2} e_{rz} \frac{\partial T}{\partial z} - \frac{\alpha_0}{2G_0\mu_0} (3\lambda_0 + 2\mu_0) \exp(\chi T) \frac{\partial T}{\partial r} (1 + 2T) &= 0 \\ \nabla^2 w + \frac{\partial^2 u}{\partial r \partial z} + e_{rz} \frac{\partial T}{\partial r} + \frac{\partial w}{\partial z} \frac{\partial T}{\partial z} + \frac{\lambda_0}{2G_0\mu_0} \left(\frac{\partial e}{\partial z} + e \frac{\partial T}{\partial z} \right) - \frac{\alpha_0}{2G_0\mu_0} (3\lambda_0 + 2\mu_0) \exp(\chi T) \frac{\partial T}{\partial z} (1 + 2T) + \frac{1}{r} \frac{\partial u}{\partial z} &= 0 \end{aligned} \tag{5}$$

where

$$\nabla^2 = \frac{\partial^2}{\partial r^2} + \frac{1}{r} \frac{\partial}{\partial r} + \frac{\partial^2}{\partial z^2} \tag{6}$$

The solution of Eq. (5) without body forces can be expressed by the Goodier's thermoelastic displacement potential ϕ and the Boussinesq harmonic functions φ and ψ as:

$$u = \frac{\partial \phi}{\partial r} + \frac{\partial \varphi}{\partial r} + z \frac{\partial \psi}{\partial r}, \quad w = \frac{\partial \phi}{\partial z} + \frac{\partial \varphi}{\partial z} + z \frac{\partial \psi}{\partial z} - (3 - 4\nu)\psi \tag{7}$$

In which the three functions must satisfy the conditions

$$\nabla^2 \phi = K \tau, \quad \nabla^2 \varphi = 0 \quad \text{and} \quad \nabla^2 \psi = 0 \tag{8}$$

where $K(T) = \frac{(1+\nu)}{(1-\nu)} \alpha_r(T)$ is the restraint coefficient and $\tau = T - T_0$, in which T_0 is the surrounding temperature. If we take

$$-\int (\varphi + z \psi) dz = M \tag{9}$$

In the above Eq. (7), Michell's function M may be used instead of Boussinesq harmonic functions φ and ψ . Hence Eq. (7) reduces to

$$u = \frac{\partial \phi}{\partial r} - \frac{\partial^2 M}{\partial r \partial z}, \quad w = \frac{\partial \phi}{\partial z} + 2(1-\nu)\nabla^2 M - \frac{\partial^2 M}{\partial z^2} \quad (10)$$

In which Michell's function M must satisfy the condition

$$\nabla^2 \nabla^2 M = 0 \quad (11)$$

Now by using Eq. (10) in Eq. (4), the results for stresses are obtained as:

$$\begin{aligned} \sigma_{rr} &= \exp(\varpi T) \left\{ 2G_0 \frac{\partial}{\partial r} \left(\frac{\partial \phi}{\partial r} - \frac{\partial^2 M}{\partial r \partial z} \right) + \lambda_0 \left[\nabla^2 \phi + (1-2\nu) \frac{\partial}{\partial z} (\nabla^2 M) \right] - (3\lambda_0 + 2\mu_0) \alpha_0 \exp(\chi T) T \right\} \\ \sigma_{\theta\theta} &= \exp(\varpi T) \left\{ 2G_0 \frac{1}{r} \left(\frac{\partial \phi}{\partial r} - \frac{\partial^2 M}{\partial r \partial z} \right) + \lambda_0 \left[\nabla^2 \phi + (1-2\nu) \frac{\partial}{\partial z} (\nabla^2 M) \right] - (3\lambda_0 + 2\mu_0) \alpha_0 \exp(\chi T) T \right\} \\ \sigma_{zz} &= \exp(\varpi T) \left\{ 2G_0 \frac{\partial}{\partial z} \left(\frac{\partial \phi}{\partial z} + 2(1-\nu)\nabla^2 M - \frac{\partial^2 M}{\partial z^2} \right) + \lambda_0 \left[\nabla^2 \phi + (1-2\nu) \frac{\partial}{\partial z} (\nabla^2 M) \right] \right\} \\ &\quad - (3\lambda_0 + 2\mu_0) \alpha_0 \exp(\varpi T) \exp(\chi T) T \\ \sigma_{rz} &= \exp(\varpi T) G_0 \left[\frac{\partial}{\partial z} \left(\frac{\partial \phi}{\partial r} - \frac{\partial^2 M}{\partial r \partial z} \right) + \frac{\partial}{\partial r} \left(\frac{\partial \phi}{\partial z} + 2(1-\nu)\nabla^2 M - \frac{\partial^2 M}{\partial z^2} \right) \right] \end{aligned} \quad (12)$$

The boundary conditions on the traction free surface stress functions are

$$\sigma_{rz} \Big|_{r=b} = \sigma_{rz} \Big|_{z=0} = \sigma_{rz} \Big|_{z=h} = 0 \quad (13)$$

3 HEAT CONDUCTION EQUATION AND ITS SOLUTION

We consider the temperature dependent transient heat conduction equation with initial and boundary conditions in a hollow cylinder given by

$$\frac{1}{r} \frac{\partial}{\partial r} \left(r k(z, T) \frac{\partial T}{\partial r} \right) + \frac{\partial}{\partial z} \left(k(z, T) \frac{\partial T}{\partial z} \right) + g(r, z, t) = C(z, T) \frac{\partial T}{\partial t} \quad (14)$$

$$T = T_0, \quad \text{at } t = 0 \quad (15)$$

$$\begin{aligned} k(z, T) \frac{\partial T}{\partial r} &= e_1 (T - T_0), \quad \text{at } r = a \\ k(z, T) \frac{\partial T}{\partial r} &= -e_2 (T - T_0), \quad \text{at } r = b \\ k(z, T) \frac{\partial T}{\partial z} &= f(r, t), \quad \text{at } z = 0 \end{aligned} \quad (16)$$

$$\frac{\partial T}{\partial z} = 0, \quad \text{at } z = h$$

where $k(z, T)$ and $C(z, T)$ are the thermal conductivity and calorific capacity, $g(r, z, t)$ is the internal heat source, T_0 is the temperature of the surrounding medium, e_1, e_2 are the heat transfer coefficients.

Introducing the Kirchhoff's variable [12, 15, 22, 23]

$$\Theta(T) = \int_{r_0}^T k(z, T) dT \tag{17}$$

and taking into account that the material with simple thermal nonlinearity ($C(z, T) / k(z, T) \approx 1$) is considered, we obtain Eq. (14) with variable Θ as:

$$\left(\frac{\partial^2 \Theta}{\partial r^2} + \frac{1}{r} \frac{\partial \Theta}{\partial r} \right) + \frac{\partial^2 \Theta}{\partial z^2} + g(r, z, t) = \frac{\partial \Theta}{\partial t} \tag{18}$$

The initial and boundary conditions are expressed as:

$$\begin{aligned} \Theta &= 0, & \text{at } t &= 0 \\ \frac{\partial \Theta}{\partial r} - e_1 \Theta_c &= 0, & \text{at } r &= a \\ \frac{\partial \Theta}{\partial r} + e_2 \Theta_c &= 0, & \text{at } r &= b \\ \frac{\partial \Theta}{\partial z} &= f(r, t), & \text{at } z &= 0 \\ \frac{\partial \Theta}{\partial z} &= 0, & \text{at } z &= h \end{aligned} \tag{19}$$

where Θ_c is the temperature determined in terms of the Kirchhoff variable from relation (17).

To complete the linearization of the conditions of convective heat transfer (19), we carry out the change of variable $\Theta_c = (1 + \nu)\Theta$, where ν is an unknown constant. Following [6], for $\nu = 0$, the conditions (19) becomes

$$\begin{aligned} \Theta &= 0, & \text{at } t &= 0 \\ \frac{\partial \Theta}{\partial r} - e_1 \Theta &= 0, & \text{at } r &= a \\ \frac{\partial \Theta}{\partial r} + e_2 \Theta &= 0, & \text{at } r &= b \\ \frac{\partial \Theta}{\partial z} &= f(r, t), & \text{at } z &= 0 \\ \frac{\partial \Theta}{\partial z} &= 0, & \text{at } z &= h \end{aligned} \tag{20}$$

For the sake of brevity, we take $g(r, z, t) = Q_1 \delta(r - r_0) \delta(z - z_0) \sinh(\gamma_1 t)$, $f(r, t) = Q_2 \delta(r - r_0) \sin(\gamma_2 t)$. Using the transform given in [11] to solve Eq. (18) with the aid of boundary conditions given by Eq. (20), we obtain

$$-q_i^2 \bar{\Theta} + \frac{\partial^2 \bar{\Theta}}{\partial z^2} + \bar{g}(q_i, z, t) = \frac{\partial \bar{\Theta}}{\partial t} \tag{21}$$

The initial and boundary conditions are

$$\begin{aligned} \bar{\Theta} &= 0, & \text{at } t &= 0 \\ \frac{\partial \bar{\Theta}}{\partial z} &= \bar{f}(q_i, t), & \text{at } z &= 0 \\ \frac{\partial \bar{\Theta}}{\partial z} &= 0, & \text{at } z &= h \end{aligned} \tag{22}$$

where $\bar{g}(q_i, z, t) = Q_1 r_0 S(q_i r_0) \delta(z - z_0) \sinh(\gamma_1 t)$, $\bar{f}(q_i, t) = Q_2 r_0 S(q_i r_0) \sin(\gamma_2 t)$. Here $S(q_i r)$ is the kernel of the transformation given by $S(q_i r) = [B(q_i a, -e_1) + B(q_i b, e_2)] J_0(q_i r) - [A(q_i a, -e_1) + A(q_i b, e_2)] Y_0(q_i r)$.

In which

$$A(q_i r, e_i) = e_i J_0(q_i r) + q_i J_0'(q_i r); \quad i = 1, 2; \quad r = a, b$$

$$B(q_i r, e_i) = e_i Y_0(q_i r) + q_i Y_0'(q_i r); \quad i = 1, 2; \quad r = a, b$$

Here J_0 and Y_0 are Bessel's function of first kind and second kind respectively and q_i are the positive roots of the transcendental equation $B(q_i a, -e_1) \times A(q_i b, e_2) - A(q_i a, -e_1) \times B(q_i b, e_2) = 0$.

Now applying finite Fourier Cosine transform on Eq. (21) and using the conditions from Eq. (22), we obtain

$$\frac{\partial \bar{\Theta}}{\partial t} + A_1 \bar{\Theta} + A_2 \sin(\gamma_2 t) - A_3 \sinh(\gamma_1 t) = 0 \quad (23)$$

The initial condition is

$$\bar{\Theta} = 0, \quad \text{at } t = 0 \quad (24)$$

where $A_1 = (q_i^2 + \beta_n^2)$, $A_2 = Q_2 r_0 S(q_i r_0)$, $A_3 = (Q_1 r_0 / k_0) S(q_i r_0) z_0 \cos(n\pi z_0 / h)$, $\beta_n = (n\pi / h)$, n is the transform parameter, the kernel being $\cos(n\pi z / h)$ and applying Laplace Transform and its inverse on Eqs. (23) and (24), we obtain

$$\bar{\Theta}(n, t) = (E_1 - E_4) \exp(-A_1 t) + E_2 \exp(-\gamma_1 t) + E_3 \exp(\gamma_1 t) + E_4 \cos(\gamma_2 t) - E_5 \sin(\gamma_2 t) \quad (25)$$

where

$$E_1 = \frac{A_3 \gamma_1}{A_1^2 - \gamma_1^2}, \quad E_2 = \frac{A_3}{2\gamma_1 - 2A_1}, \quad E_3 = \frac{A_3}{2\gamma_1 + 2A_1}, \quad E_4 = \frac{A_2 \gamma_2}{A_1^2 + \gamma_2^2}, \quad E_5 = \frac{A_1 A_2}{A_1^2 + \gamma_2^2}$$

Applying inverse Fourier Cosine transform on Eq. (25), we obtain

$$\bar{\Theta}(z, t) = \frac{[\bar{\Theta}(n, t)]_{n=0}}{h} + \frac{2}{h} \sum_{n=1}^{\infty} \{\bar{\Theta}(n, t) \cos(n\pi z / h)\}$$

Taking inverse transform defined in [11] on the above equation, we obtain

$$\Theta(r, z, t) = \sum_{i=1}^{\infty} \frac{\bar{\Theta}(z, t)}{S(q_i)} S(q_i r)$$

where $S(q_i) = \int_a^b r S(q_i r) S(q_j r) dr$, $i = j$

$$\Theta(r, z, t) = \sum_{i=1}^{\infty} \{ \{ [\bar{\Theta}(n, t)]_{n=0} / h \} + (2/h) \sum_{n=1}^{\infty} \{ \bar{\Theta}(n, t) \cos(n\pi z / h) \} \} \times [\xi_1 J_0(q_i r) - \xi_2 Y_0(q_i r)] \quad (26)$$

where $\xi_1 = [B(q_i a, -e_1) + B(q_i b, e_2)] / S(q_i)$, $\xi_2 = [A(q_i a, -e_1) + A(q_i b, e_2)] / S(q_i)$

Applying variable inverse transformation from Θ to T (See Appendix A), the temperature distribution in Eq. (26) becomes

$$T(r, z, t) \cong T_0 + \sum_{i=1}^{\infty} (1/\exp(\varpi T_0)) \{ [1/u(z)] \{ [\bar{\Theta}(n, t)]_{n=0} / h \} + (2/h) \sum_{n=1}^{\infty} \{ \bar{\Theta}(n, t) \cos(n\pi z / h) \} \} \times [\xi_1 J_0(q_i r) - \xi_2 Y_0(q_i r)] \tag{27}$$

where $u(z) = [f_m(z)(k_{m_0} - k_{c_0}) + k_{c_0}]$, $f_m(z) = 1 - z^d$.

4 THERMOELASTIC ANALYSIS

Referring to the heat conduction Eq. (14) and its solution given by Eq. (27), the solution for the Goodier's thermoelastic displacement potential ϕ governed by Eq. (8) is obtained as:

$$\phi = \sum_{i=1}^{\infty} \sum_{n=1}^{\infty} \{ \{ K [(2/h^2)] Q_1 r_0 S(q_i r_0) \sin(\gamma_2 t) g_1(z) + (2/h) \bar{\Theta}(n, t) g_2(z) \}^2 / [-q_i^2 g_3(z)] \times [\xi_1 J_0(q_i r) - \xi_2 Y_0(q_i r)] \} - \{ K f_1(r, z) [(2/h^2)] Q_1 r_0 S(q_i r_0) \sin(\gamma_2 t) g_1(z) + (2/h) \bar{\Theta}(n, t) g_2(z) \} / [-q_i^2 g_3(z)] \} \} \tag{28}$$

where

$$g_1(z) = ([\bar{\Theta}(n, t)]_{n=0} / h) / u(z), \quad g_2(z) = \cos(n\pi z / h) / u(z), \\ g_3(z) = (2/h^2) Q_1 r_0 S(q_i r_0) \sin(\gamma_2 t) [g_1(z) + g_1''(z)] + (2/h) \bar{\Theta}(n, t) [g_1(z) + g_1''(z)]$$

Similarly, the solution for Michell's function M assumed so as to satisfy the governed condition of Eq. (12) is obtained as:

$$M = \sum_{i=1}^{\infty} \sum_{n=1}^{\infty} \{ \cos(n\pi z / L) \exp(\psi t) [C_n J_0(q_i r) + D_n r Y_0(q_i r)] \} \tag{29}$$

where C_n and D_n are constants. Now, in order to obtain the displacement components, we substitute the values of ϕ and M in Eq. (10), and obtain

$$u = \sum_{i=1}^{\infty} \sum_{n=1}^{\infty} \{ \phi_{,r} + [(n\pi / L) \cos(n\pi z / L) \exp(\psi t)] \times [-C_n q_i J_1(q_i r) - D_n r q_i Y_1(q_i r) + D_n Y_0(q_i r)] \} \tag{30}$$

$$w = \sum_{i=1}^{\infty} \sum_{n=1}^{\infty} \{ \phi_{,z} + [(2-2\nu) \cos(n\pi z / L) \exp(\psi t)] [-C_n q_i^2 J_0(q_i r) + D_n Y_0(q_i r)] (1/r - q_i r) \} + [(1-2\nu)(-n^2 \pi^2 / L^2) \cos(n\pi z / L) \exp(\psi t) [C_n J_0(q_i r) + D_n r Y_0(q_i r)]] \} \tag{31}$$

where a comma denotes differentiation with respect to the following variable.

Using the displacement components given by Eqs. (30) and (31) in Eq. (12), the components of stresses in the homogeneous (by taking $\varpi = \chi = 0$) as well as nonhomogeneous case (by taking $\varpi \neq \chi \neq 0$) may be obtained. Also by using the traction free conditions given by Eq. (13) the constants C_n and D_n may be determined.

5 NUMERICAL RESULTS AND DISCUSSION

Following [11], we consider a model of a ceramic-metal-based FGM, in which alumina is selected as the ceramic and nickel as the metal.

Table 1

Thermo-mechanical properties of alumina and nickel at room temperature.

Property	Alumina (Ceramic)	Nickel (Metal)
Thermal conductivity k [W/cmK]	0.282	0.901
Thermal diffusivity k [$\times 10^{-6} \text{cm}^2/\text{s}$]	0.083	0.223
Thermal expansion coefficient α [$\times 10^{-6}/\text{K}$]	5.4	14.0
Young's modulus E [N/cm ²]	36×10^6	21.8×10^6
Poisson's ratio ν	0.23	0.31

For numerical computations, we introduce the following non-dimensional parameters.

$$\bar{T} = \frac{T}{T_0}, \quad \eta = \frac{r}{h}, \quad \zeta = \frac{z}{h}, \quad \tau = \frac{\kappa t}{h^2}, \quad (\bar{u}, \bar{w}) = \frac{(u, w)}{K_0 T_0 h},$$

$$K_0 = \frac{1+\nu}{1-\nu} \alpha_0, \quad (\bar{\sigma}_{rr}, \bar{\sigma}_{\theta\theta}, \bar{\sigma}_{zz}, \bar{\sigma}_{rz}) = \frac{(\sigma_{rr}, \sigma_{\theta\theta}, \sigma_{zz}, \sigma_{rz})}{E_0 \alpha_0 T_0}$$

with parameters $a = 1 \text{cm}$, $b = 2 \text{cm}$, $h = 2 \text{cm}$, $t = 2 \text{sec}$, Surrounding Temperature $T_0 = 320^\circ \text{K}$.

The Figs. (1 to 7) on the left are plotted along radial direction, whereas the figures on the right are plotted along axial direction. Fig. 1 shows the variation of dimensionless temperature along radial and axial directions for different values of $\zeta = 0.25, 0.5, 1$ and $\eta = 0.5, 0.75, 1$ respectively. Along radial direction, it is seen that, there is some heat initially due to surrounding temperature and the absolute value of temperature is decreasing as the heat is transferred from the curved surface towards the inner radius. Thermal energy is accumulated near the point $\eta = 0.8$ and hence all the points of ζ are coinciding. Also since sectional heating is given at the upper surface, the magnitude of temperature is high and is slowly decreasing towards the lower surface. Along axial direction, it is seen that the absolute value of temperature is high at the upper surface and is slowly decreasing till $\zeta = 0.4$. The accumulation of thermal energy at $\zeta = 0.7$ is causing the temperature to raise a little towards the lower surface.

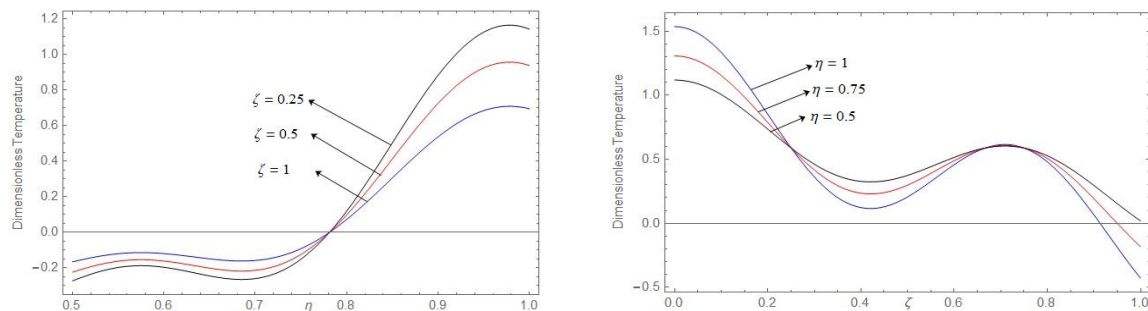


Fig.1

Variation of dimensionless temperature along radial and axial directions.

Fig. 2 shows the variation of dimensionless displacement \bar{u} along radial and axial directions for different values of ζ and η respectively. Along radial direction, it is seen that the nature of the graph is sinusoidal. The magnitude of displacement is slowly and steadily increasing from the outer curved surface till $\eta = 0.78$, and suddenly decreasing towards the central part of the cylinder and is becoming zero at the inner radius. Along axial direction, it is seen that the absolute value of displacement nearly zero at the upper surface and is suddenly increasing towards the lower surface in the region $0.6 < \zeta < 1$.

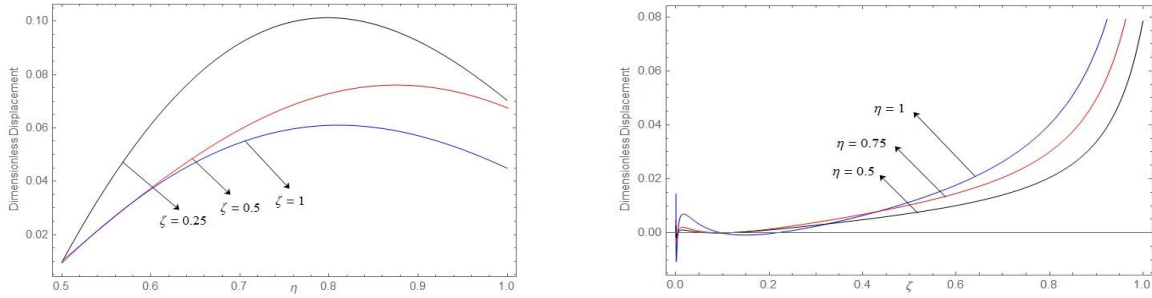


Fig.2
Variation of dimensionless displacement \bar{u} along radial and axial directions.

Fig. 3 shows the variation of dimensionless displacement \bar{w} along radial and axial directions for different values of ζ and η respectively. Along radial direction, it is seen that the displacement is increasing from the curved surface till $\eta = 0.82$, and suddenly decreasing towards the inner radius. Along axial direction, it is seen that displacement is more in the region $0.5 < \zeta < 0.7$, due to energy accumulation.

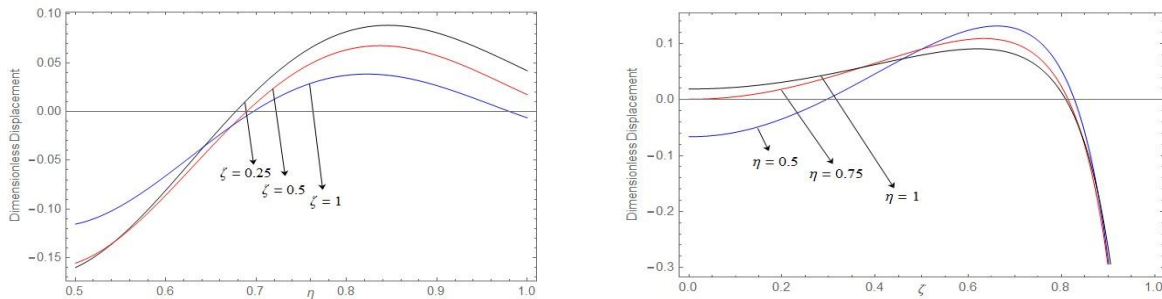


Fig.3
Variation of dimensionless displacement \bar{w} along radial and axial directions.

Fig. 4 shows the variation of dimensionless stresses along radial and axial directions for different values of ζ and η respectively in the homogeneous case. Along radial direction, it is seen that the axial stress is tensile throughout the cylinder, whereas radial and tangential stresses are compressive in the region $0.8 < \eta < 1$ and tensile in $0.5 < \eta < 0.8$. The magnitude of stresses is near the inner radius is high due to heat transfer from the curved surface to inner radius. Along axial direction, the axial stress is tensile in the region $0.6 < \zeta < 1$, whereas compressive for the rest of the region. The radial and tangential stresses are compressive in the region $0 < \zeta < 0.7$, whereas tensile towards the lower surface.

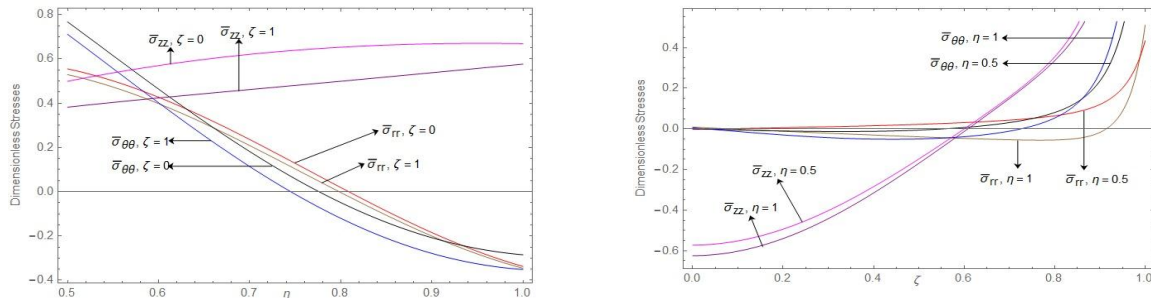


Fig.4
Variation of dimensionless stresses along radial and axial directions in the homogeneous case.

Fig. 5 shows the variation of dimensionless stresses along radial and axial directions for different values of ζ and η respectively in the nonhomogeneous case. Along radial direction, it is seen that all the stresses are

compressive throughout the cylinder. The absolute value of radial and axial stresses in slowly increasing from the curved surface towards the inner radius, whereas for tangential stress it is more or less same. Along axial direction, it is seen that all the stresses are compressive throughout the cylinder. The absolute value of all the stresses is nearly steady near the upper surface, while suddenly declining towards the lower surface.

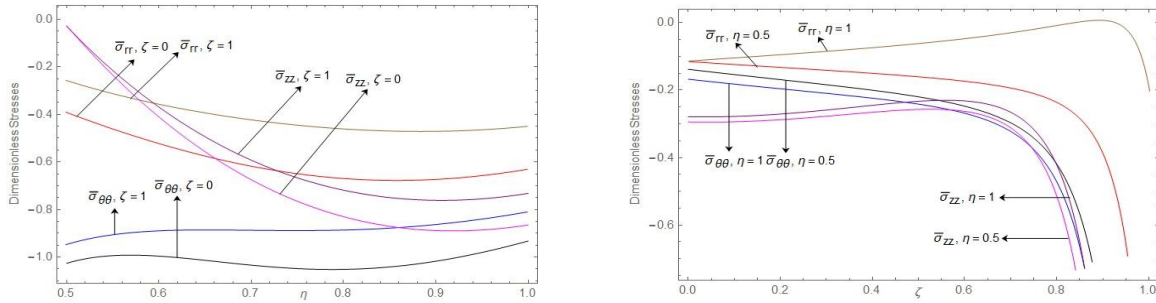


Fig.5
Variation of dimensionless stresses along radial and axial directions in the nonhomogeneous case.

Fig. 6 shows the variation of dimensionless shear stress along radial and axial directions for different values of ζ and η respectively in the homogeneous case. Along radial direction, it is observed that the shear stress is compressive throughout the cylinder. Along axial direction, it is compressive in the region $0 < \zeta < 0.6$, whereas tensile towards the lower surface.

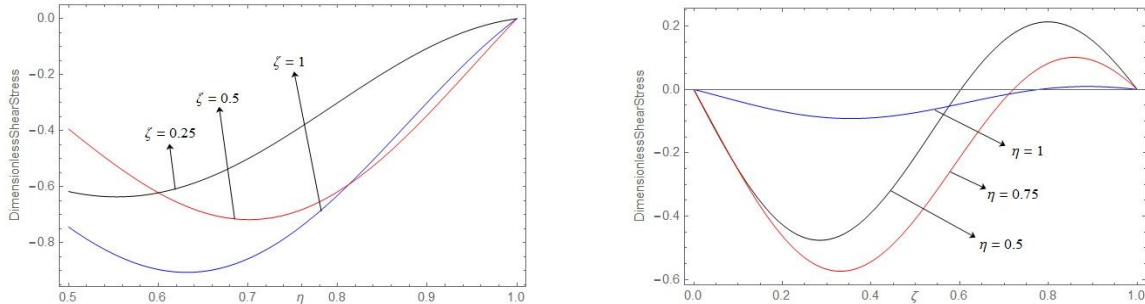


Fig.6
Variation of dimensionless shear stress along radial and axial directions in the homogeneous case.

Fig. 7 shows the variation of dimensionless shear stress along radial and axial directions for different values of ζ and η respectively in the nonhomogeneous case. Along radial direction, it is observed that the shear stress is compressive throughout the cylinder. Its absolute value is decreasing from the curved surface till $\eta = 0.6$ and suddenly increasing towards the inner radius. Along axial direction, the shear stress is compressive throughout the cylinder. Its absolute value is decreasing from the upper surface till $\zeta = 0.4$ and suddenly increasing towards the lower surface. The shear stress is zero at both surfaces satisfying the prescribed traction free conditions.

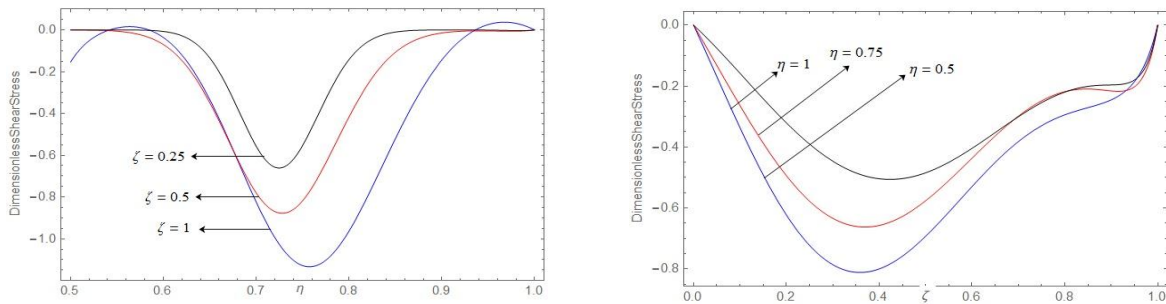


Fig.7
Variation of dimensionless shear stress along radial and axial directions in the nonhomogeneous case.

6 CONCLUSIONS

In the present paper, we have investigated temperature and thermal stresses in a thick hollow cylinder subjected to sectional heating on the upper surface with temperature dependent material properties. We have obtained the solution for transient two-dimensional conductivity equation with internal heat source and its associated thermal stresses for a thick hollow cylinder. The solutions are obtained in the form of Bessel's and trigonometric functions. Numerical computations are carried out for ceramic-metal-based FGM, in which alumina is selected as ceramic and nickel as metal. Furthermore the influence of thermo-sensitivity on thermal stresses is investigated.

During this analysis, we observe that:

1. The nature of temperature distribution and displacement is sinusoidal along radial and axial directions.
2. The radial, axial and tangential stresses are both compressive and tensile in the homogeneous case, whereas compressive in the nonhomogeneous case.
3. The nature of shear stress is sinusoidal in both homogeneous and nonhomogeneous cases.
4. This type of theoretical analysis may be used under high temperature conditions in non-homogeneous and functionally graded materials.

From the above observations one can conclude that there are variations in radial, tangential and axial stresses for homogeneous and nonhomogeneous cases in radial and axial directions. Also tremendous change is seen in shear stress in both homogeneous and nonhomogeneous cases for both radial and axial directions. These variations are due to the presence of inhomogeneity parameters ϖ, χ .

APPENDIX A

The volume fraction distribution of metal obeying simple power law with exponent d is given as: [8]

$$f_m(z) = 1 - z^d \quad \text{for } d \geq 0 \tag{A.1}$$

where $f_m(z)$ is the local volume fraction of metal in a functionally graded plate and d is a parameter that describes the volume fraction of metal.

We express the thermal conductivity of the material using the thermal conductivities of metals k_m and of ceramics k_c with the volume fractions of metals $f_m(z)$, and ceramics, $1 - f_m(z)$ as follows:

$$k(z, T) = k_m(T)f_m(z) + k_c(T)(1 - f_m(z)) \tag{A.2}$$

Inverse transformation: We substitute Eq. (A.2) in Eq. (17) to obtain the inverse transformation of Eq. (17) as:

$$\Theta(T) = \int_{T_0}^T (k_m(T)f_m(z) + k_c(T)(1 - f_m(z)))dT \tag{A.3}$$

$$\Theta(T) = f_m(z) \int_{T_0}^T k_m(T)dT + (1 - f_m(z)) \int_{T_0}^T k_c(T)dT \tag{A.4}$$

Following [4], we assume the thermal conductivity of the hollow cylinder as $k(T) = k_0 \exp(\varpi T)$.

Hence Eq. (A.4) becomes

$$\Theta = (1/\varpi)[[\exp(\varpi T) - \exp(\varpi T_0)]u(z)] \tag{A.5}$$

where $u(z) = [f_m(z)(k_{m_0} - k_{c_0}) + k_{c_0}]$. Using Eq. (A.5) in Eq. (26), we obtain,

$$T(r, z, t) = \frac{1}{\varpi} \log_e [L(r, z, t) + \exp(\varpi T_0)] = \frac{1}{\varpi} \log_e \left[\exp(\varpi T_0) \left(1 + \frac{L(r, z, t)}{\exp(\varpi T_0)} \right) \right] \tag{A.6}$$

where

$$L(r, z, t) = \sum_{i=1}^{\infty} \{[\varpi / u(z)] \{([\bar{\Theta}(n, t)]_{n=0} / h) + (2/h) \sum_{n=1}^{\infty} \{\bar{\Theta}(n, t) \cos(n \pi z / h)\}\} \times [\xi_1 J_0(q_i r) - \xi_2 Y_0(q_i r)]\} \quad (\text{A.7})$$

We use the following logarithmic expansion

$$\log_e [(L(r, z, t) / \exp(\varpi T_0)) + 1] = [L(r, z, t) / \exp(\varpi T_0)] + (1/2) [(L(r, z, t) / \exp(\varpi T_0))^2] + (1/3) [(L(r, z, t) / \exp(\varpi T_0))^3] + (1/4) [(L(r, z, t) / \exp(\varpi T_0))^4] + \dots \quad (\text{A.8})$$

We observe that $[L(r, z, t) / \exp(\varpi T_0)]^m$ given in Eq. (A.7) converges to zero as m tends to infinity. Also the truncation error in Eq. (A.8) is observed as 5.37×10^{-6} .

Hence, for the sake of brevity, neglecting the terms with order more than one, we obtain

$$\log_e [(L(r, z, t) / \exp(\varpi T_0)) + 1] \cong [L(r, z, t) / \exp(\varpi T_0)]$$

Hence Eq. (A.6) becomes

$$T(r, z, t) \cong T_0 + \sum_{i=1}^{\infty} (1 / \exp(\varpi T_0)) \{[1 / u(z)] \{([\bar{\Theta}(n, t)]_{n=0} / h) + (2/h) \sum_{n=1}^{\infty} \{\bar{\Theta}(n, t) \cos(n \pi z / h)\}\} \times [\xi_1 J_0(q_i r) - \xi_2 Y_0(q_i r)]\}$$

REFERENCES

- [1] Al-Hajri M., Kalla S. L., 2004, On an integral transform involving Bessel functions, *Proceedings of the International Conference on Mathematics and its Applications*, Kuwait.
- [2] Awaji H., Takenaka H., Honda S., Nishikawa T., 2001, Temperature/Stress distributions in a stress-relief-type plate of functionally graded materials under thermal shock, *JSME International Journal Series A Solid Mechanics and Material Engineering* **44**: 1059-1065.
- [3] Ching H. K., Chen J. K., 2007, Thermal stress analysis of functionally graded composites with temperature-dependent material properties, *Journal of Mechanics of Materials and Structures* **2**: 633-653.
- [4] Farid M., Zahedinejad P., Malekzadeh P., 2010, Three-dimensional temperature dependent free vibration analysis of functionally graded material curved panels resting on two-parameter elastic foundation using a hybrid semi-analytic differential quadrature method, *Materials & Design* **31**: 2-13.
- [5] Hata T., 1982, Thermal stresses in a non-homogeneous thick plate under steady distribution of temperature, *Journal of Thermal Stresses* **5**: 1-11.
- [6] Hosseini S. M., Akhlaghi M., 2009, Analytical solution in transient thermo-elasticity of functionally graded thick hollow cylinders, *Mathematical Methods in the Applied Sciences* **32**: 2019-2034.
- [7] Kassir K., 1972, Boussinesq problems for non-homogeneous solid, *Proceedings of the American Society of Civil Engineers Definition, Journal of the Engineering Mechanics Division* **98**: 457-470.
- [8] Kumar R., Devi Sh., Sharma V., 2017, Axisymmetric problem of thick circular plate with heat sources in modified couple stress theory, *Journal of Solid Mechanics* **9**: 157-171.
- [9] Kumar R., Manthana V.R., Lamba N.K., Kedar G.D., 2017, Generalized thermoelastic axi-symmetric deformation problem in a thick circular plate with dual phase lags and two temperatures, *Material Physics and Mechanics* **32**: 123-132.
- [10] Kushnir R. M., Protsyuk Yu., 2008, Thermal stressed state of layered thermally sensitive cylinders and spheres under the conditions of convective-radiation heat transfer, *Mathematical Modeling Inform Technology* **40**: 103-112.
- [11] Kushnir R. M., Popovych V.S., 2011, *Heat Conduction Problems of Thermo-Sensitive Solids under Complex Heat Exchange*, Intech.
- [12] Lamba N.K., Walde R.T., Manthana V.R., Khobragade N.W., 2012, Stress functions in a hollow cylinder under heating and cooling Process, *Journal of Statistics and Mathematics* **3**: 118-124.
- [13] Liew K. M., Kitipornchai S., Zhang X. Z., Lim C. W., 2003, Analysis of the thermal stress behaviour of functionally graded hollow circular cylinders, *The International Journal of Solids and Structures* **40**: 2355-2380.

- [14] Manthana V.R., Lamba N.K., Kedar G.D., 2016, Spring backward phenomenon of a transversely isotropic functionally graded composite cylindrical shell, *Journal of Applied and Computational Mechanics* **2**: 134-143.
- [15] Manthana V.R., Lamba N.K., Kedar G.D., 2017, Thermal stress analysis in a functionally graded hollow elliptic-cylinder subjected to uniform temperature distribution, *Applications and Applied Mathematics* **12**: 613-632.
- [16] Manthana V.R., Kedar G.D., 2017, Transient thermal stress analysis of a functionally graded thick hollow cylinder with temperature dependent material properties, *Journal of Thermal Stresses* **41**: 568-582.
- [17] Manthana V.R., Lamba N.K., Kedar G.D., 2018, Mathematical modeling of thermoelastic state of a thick hollow cylinder with nonhomogeneous material properties, *Journal of Solid Mechanics* **10**: 142-156.
- [18] Manthana V.R., Lamba N.K., Kedar G.D., 2018, Thermoelastic analysis of a rectangular plate with nonhomogeneous material properties and internal heat source, *Journal of Solid Mechanics* **10**: 200-215.
- [19] Moosaie A., 2012, Steady symmetrical temperature field in a hollow spherical particle with temperature-dependent thermal conductivity, *Archives of Mechanics* **64**: 405-422.
- [20] Moosaie A., 2015, Axisymmetric steady temperature field in FGM cylindrical shells with temperature-dependent heat conductivity and arbitrary linear boundary conditions, *Archives of Mechanics* **67**: 233-251.
- [21] Noda N., 1991, Thermal stresses in materials with temperature dependent properties, *Applied Mechanics Reviews* **44**: 383-397.
- [22] Peng X. L., Li X. F., 2010, Thermo-elastic analysis of a cylindrical vessel of functionally graded materials, *International Journal of Pressure Vessels Piping* **87**: 203-210.
- [23] Popovych V. S., 1990, Modeling of heat fields in thin thermo-sensitive plates, *Modeling and Optimization of Complex Mechanical Systems* **1990**: 70-75.
- [24] Popovych V. S., Garmatii G. Yu., 1993, Analytic-numerical methods of constructing solutions of heat-conduction problems for thermo-sensitive bodies with convective heat transfer, *Pidstrigach Institute for Applied Problems of Mechanics and Mathematics* **1993**: 13-93.
- [25] Popovych V. S., Fedai B. N., 1997, The axi-symmetric problem of thermo-elasticity of a multilayer thermo-sensitive tube, *Journal of Mathematical Sciences* **86**: 2605-2610.
- [26] Popovych V. S., Makhorkin I. M., 1998, On the solution of heat-conduction problems for thermo-sensitive bodies, *Journal of Mathematical Sciences* **88**: 352-359.
- [27] Popovych V. S., Kalynyak B. M., 2005, Thermal stressed state of a thermally sensitive cylinder in the process of convective heating, *Mathematics Metody Fiz Mekh Polya* **48**: 126-136.
- [28] Popovych V. S., Harmatii H. Yu., Vovk O. M., 2006, Thermoelastic state of a thermo-sensitive space with a spherical cavity under convective-radiant heat exchange, *Mathematics Metody Fiz Mekh Polya* **49**: 168-176.
- [29] Popovych V. S., 2014, Methods for determination of the thermo-stressed state of thermally sensitive solids under complex heat exchange conditions, *Encyclopedia of Thermal Stresses* **6**: 2997-3008.
- [30] Popovych V. S., Kalynyak B. M., 2016, Mathematical modeling and methods for the determination of the static thermoelastic state of multilayer thermally sensitive cylinders, *Journal of Mathematical Sciences* **215**: 218-242.
- [31] Rakocha I., Popovych V. S., 2016, The mathematical modeling and investigation of the stress-strain state of the three-layer thermosensitive hollow cylinder, *Acta Mechanica et Automatica* **10**: 181-188.
- [32] Tang S., 1968, Thermal stresses in temperature dependent isotropic plates, *Journal of Spacecrafts and Rockets* **5**: 987-990.
- [33] Thawait A.K., Sondhi L., Sanyal Sh., Bhowmick Sh., 2017, Elastic analysis of functionally graded variable thickness rotating disk by element based material grading, *Journal of Solid Mechanics* **9**: 650-662.
- [34] Tripathi J. J., Kedar G. D., Deshmukh K. C., 2017, Generalized thermoelastic problem of a thick circular plate with axisymmetric heat supply due to internal heat generation, *Journal of Solid Mechanics* **9**: 115-125.